Chapter 11
Neutron Imaging for the Hydrogen Economy

M. Arif, D.S. Hussey, and D.L. Jacobson

Abstract The development of fuel cells and hydrogen storage materials will be one of the highest global research and development priorities for the foreseeable future. The particular abilities of neutrons to penetrate materials and to image hydrogen will make neutron imaging a key technique, allowing the in-situ study of real operational devices. This chapter describes the current state of the art in this field.

Keywords Fuel cell · PEM · Hydrogen storage · Water dynamics

11.1 Introduction

Compared to most other forms of radiation, neutrons are highly efficient means of probing complex structures because of their tremendous of penetrating capability many common materials and their unique capability of distinguishing different materials with similar chemical and physical properties. Consequently, neutron imaging has always been regarded as one of the most potentially important tools for many areas of industrial research. However, these promises have remained largely unfulfilled, and neutron imaging techniques have seen limited applications, primarily due to traditionally poor spatial resolution and slow processing time as well as lack of identification of critical, high-impact areas of research. Most industrial and academic research that can significantly benefit from this technique involves dimensions that are a few tens of micrometers in length and interaction times that last at longest a few seconds. The current practical limitations for neutrons are about 100 μm in spatial resolution and tens of seconds in time resolution. These limitations are mainly due to the relatively weak neutron sources (nuclear reactors that are many orders of magnitude weaker than even table-top photon sources), large mean free paths of neutrons and secondary radiation in

M. Arif (✉)
National Institute of Standards and Technology, 100 Bureau Drive, MS 6100,
Gaithersburg, MD 20899-6100, USA
e-mail: muhammed.arif@nist.gov

I.S. Anderson et al. (eds.), *Neutron Imaging and Applications*,
Neutron Scattering Applications and Techniques, DOI 10.1007/978-0-387-78693-3_11,

materials (limits spatial resolution), and the inability to process data in real-time while being statistically significant (limited by weak source).

However, in the past decade enough gains have been made to enable neutron imaging to be applied in different fields of science and technology. One of the most important prospects is the understanding of the interface physics, chemical kinetics, and proper modeling of the processes that govern the operation of the future generation of energy production and storage devices based on hydrogen. The sensitivity of neutrons to hydrogen, together with other unique properties, makes them an ideal probe for characterizing the structure, morphology, and hydrogen dynamics that are key to the future use of these promising devices. The neutron imaging technique, in particular, has emerged as one of the most important tools in the development of robust and efficient fuel cells accompanying hydrogen storage materials and devices. This article will focus on the application of neutron imaging research in the development of low-temperature fuel cells that may power homes, consumer electronics, and transport vehicles in the emerging hydrogen economy.

11.2 Neutron Imaging of Fuel Cells and Hydrogen Storage Devices

11.2.1 Neutron Imaging of Fuel Cells

Fuel cells are efficient, silent, and virtually non-polluting electrochemical devices that have immense potential for powering homes, businesses, and transport vehicles of the future. Major energy-related and automobile companies worldwide are currently engaged in extensive research to perfect fuel cells for everyday, cost-efficient use.

Fuel cells containing solid proton exchange membranes (PEM) are of special interest, as they enable fuel cell operation at lower temperatures ($< 100^{\circ}C$) than conventional solid oxide fuel cells ($> 500^{\circ}C$). PEM fuel cells convert the chemical energy of hydrogen-containing fuels directly into electricity in the presence of a catalyst, without combustion and without any moving parts. Fuel cells provide a quantum leap in fuel efficiencies compared to traditional heat engines because conversion to electricity does not require the intermediate generation of heat. Similar to batteries, fuel cells generate power electrochemically and thereby produce extremely low to zero emissions, depending on the fuel supply and operating conditions.

Current PEM fuel cells use perfluorosulfonic acid-based membrane technology such as Nafion® and Gore-Select® [1]. Platinum catalyst is applied to both sides of the membrane to form the membrane electrode assembly (MEA). During operation, hydrogen gas is brought to the anode side of the MEA while air is brought to the cathode side. H_2 is oxidized to protons and electrons. The protons migrate through the membrane (Fig. 11.1) to the cathode side and react with O_2 in the air to form water. The electrons, on the other hand, conduct externally to provide electricity. In this process, water is "dragged" from the

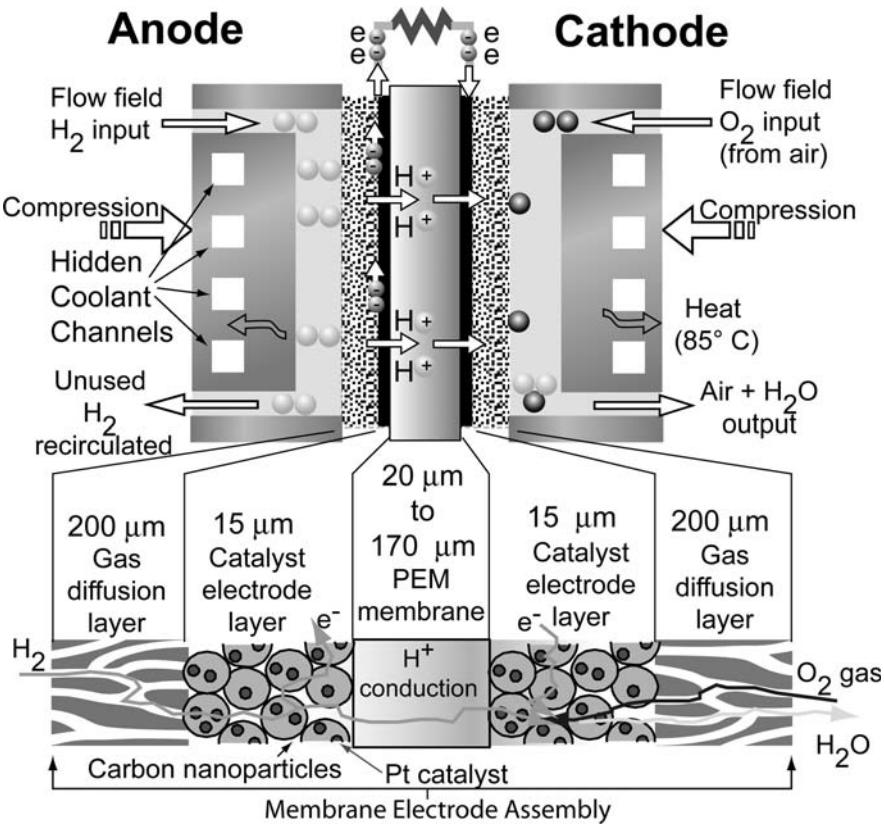

Fig. 11.1 Schematic of a fuel cell. The platinum (Pt) catalyst is generally applied to both sides of the membrane to form the membrane electrode assembly. Formation of water at the membrane can cause the cell to perform poorly

anode side of the MEA to the cathode side with the proton transport. In the meantime, water is generated on the cathode side of the MEA. A water gradient thus exists within the membrane. The PEM water content is extremely critical as it impacts the ionic conductivity and mechanical properties such as strength and gas permeability. Depending on the water concentration, the membrane performance and lifetime can be significantly reduced. In order to maintain the proton conductivity and preserve membrane life, PEM fuel cells typically require humidified reactant gases. This vapor, together with the water generated during operation, poses significant challenges for water management. A hydrophobic porous gas diffusion layer (GDL) is typically used to help manage water distribution. Furthermore, the electrode composition may be hydrophobic or hydrophilic, which is another area of water management difficulty.

PEM fuel cells have gone through significant evolution in recent years, but one of the remaining key challenges is efficient water management. The control

of incoming humidity and the product water within the MEA and GDL is generally acknowledged as one of the most crucial aspects of operating a PEM fuel cell. Too much water within the MEA or GDL will result in flooding conditions that impede gas diffusion; too little water will reduce the membrane proton conductivity, thereby decreasing the cell performance; and cycling between water levels will reduce membrane life. Thus, proper water management is the key to a stable and long-life PEM fuel cell and must be achieved by properly designing the flowfield, the GDL, the MEA, and their interfaces. This requires a fundamental understanding of the *in situ* water distribution in an operating fuel cell.

It is critically important for both optimal design and efficient operation of the fuel cells to study and quantify these adverse effects in situ using non-destructive means [2]. At present, neutron imaging is the only technology that has the ability to look inside a standard, commercially viable PEM fuel cell while the cell is operating and characterize the water content non-destructively. Since neutrons are highly penetrating in most materials, they are ideal probes in the investigation of internal structures of bulk objects like the fuel cell. Thermal neutrons (low-energy neutrons) passing through matter experience the following interactions: (a) absorption, (b) scattering (elastic, inelastic, small angle scattering), (c) refraction, (d) change in the phase of the neutron wave, (e) depolarization of an incident spin direction.

These interactions are used for signals in thermal neutron two-dimensional (2D) (radiographic) and 3D (tomographic) imaging (Chapters 5 and 6, in this volume). The most common processes are absorption and scattering. The thermal cross-sections for absorption and scattering events are complex functions of atomic mass, atomic number, nuclear isotope, and neutron energy. The contrast obtainable between materials in radiographic images is a function of their different cross-sections. For thermal neutrons, hydrogen-based compounds (such as water) would be highly visible against aluminum, iron, or carbon, which are commonly used in fuel cell construction (Fig. 6.1). This is due to the fact that the so-called mass attenuation coefficient of water is nearly two orders of magnitude larger than that of the background materials. This unique signature of hydrogen allows for the study of water transport phenomena in fuel cells with sub-microgram precision.

11.2.2 Neutron Imaging of Hydrogen Storage Devices

Vehicles powered by PEM fuel cells require, among other things, the presence of onboard hydrogen storage vessels. The design of metal-hydride beds with suitably low weight and volume to meet the demands of automotive applications is no trivial matter. The characterization of prototype technologies would benefit greatly from an in situ imaging technique such as neutron radiography to aid in understanding the hydrogen concentration gradients across these beds

during absorption/desorption cycling. As a demonstration, the hydrogen uptake in Sieverts' Reactor was imaged in situ during a hydrogen charging step. Figure 11.2 shows a photo of the Sievert's Reactor and neutron images at two different points during the hydrogen charge. Since hydrogen has such a large total neutron scattering cross-section, it is straightforward to measure the real-time metal hydride uptake of gaseous hydrogen.

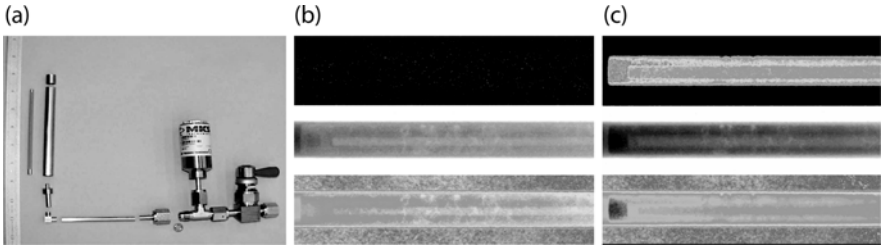

Fig. 11.2 Neutron radiography study of hydrogen storage in $LaNi_{4.78}Sn_{0.22}$. (**a**) Photo of the Sievert's reactor. (**b,c**) Colorized (*bottom*) and raw greyscale (*middle*) images of the reactor and the hydrogen content (*top*) in the uncharged and charged states, respectively

Future research on hydrogen storage will correlate local hydrogen reaction rates and contents with temperature profiles numerically simulated by detailed thermal models based on designs such as those previously developed [3,4] at the Jet Propulsion Laboratory (JPL) for hydride compressor beds to be used in sorption cryocoolers on the spacecraft of the Planck Mission [5,6]. A cross-sectional drawing of such a highly integrated hydride bed is shown in Fig. 11.3.

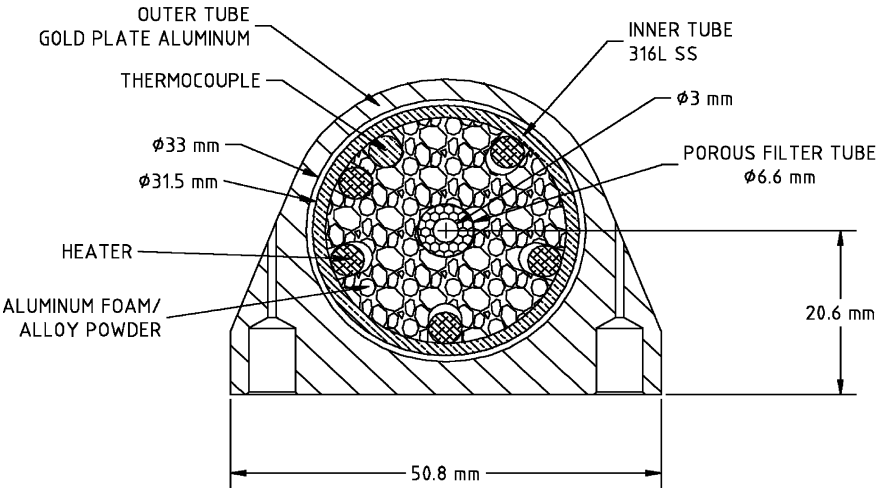

Fig. 11.3. Cross-sectional drawing of a prototype hydrogen storage bed. The porous aluminum is filled with $LaNi_{4.78}Sn_{0.22}$. With neutron tomography, the effects of hydrogen uptake, such as swelling and temperature gradients, can be revealed

This prototype hydrogen storage vessel consists of an outer aluminum shell surrounding an inner bed enclosed by a ~3 cm diameter stainless steel tube (~30 cm long) that contains an annular, open-pore Al foam matrix filled with $LaNi_{4.78}Sn_{0.22}$ hydrogen-absorbing powder. The center of the annulus contains a porous 316L stainless steel (SS) filter tube for hydrogen delivery.

In such a study, real-time images of concentration gradients within the $LaNi_{4.78}Sn_{0.22}$/Al foam hybrid matrix would need to be collected as a function of controlled stepwise hydrogen addition and removal (hydrogen coming from an adjacent control volume). Also, neutron tomography would be performed for each step after steady state had been reached. In this way, it may be possible to characterize the presence and nature of any hydrogen concentration gradients.

11.2.3 Primary Areas of Applications

11.2.3.1 Efficient Flow Field Design

Flow channels are the conduit through which hydrogen and air are drawn into a fuel cell. They also act as conduits to expel excess water. Effective design of the flow channels is essential to achieve the desired proper balance of incoming humidity and outgoing water. The design should ensure proper hydration of the MEA that in turn determines the fuel cell operating efficiency and durability. The flow channels have a typical dimension of a few tenths of a millimeter to a few millimeters and can be arranged in many different geometric patterns. By optimizing the channel geometry, efficient, passive water removal from the fuel cell can be realized, reducing the need for energy-intensive gas purges [7]. Neutron imaging has played a critical part in describing the correlation between current density and total measured water content and its distribution in operating fuel cells, since the spatial resolution of scintillators easily resolves the channel separation, as shown in Fig. 11.4.

11.2.3.2 Water Dynamics Through the PEM

Fuel cell performance depends on the complex interplay of several chemical and mass transport processes that occur at interfaces. A typical MEA consists of electrodes with catalytic particles on larger particles of a support medium, which are embedded on an electrode. Two electrodes sandwich a PEM. The structure of the electrode involves pores that have a typical length scale of 10–50 nm. For a fuel cell to be efficient, these pores must remain open for reactant transport during the operating cycle.

The first reported fuel cell neutron imaging measurement was carried out more than a decade ago [8]. It was a pioneering experiment attempting to improve the understanding of water mass transport and its effects on the electrochemical performance of PEM fuel cells via detailed knowledge of the

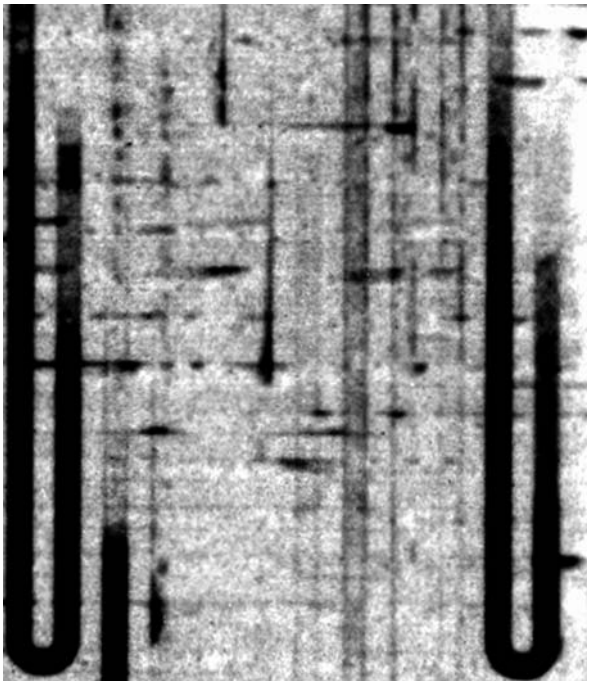

Fig. 11.4 A sub-image of a neutron radiograph of a 50 cm^2 active area fuel cell clearly showing the water content (dark areas) of the separate channels. In this case the anode and cathode channels were oriented perpendicularly to permit discrimination of anode vs. cathode channel water.

through-plane water distribution. The measurements, as shown in Fig. 11.5, involved direct neutron imaging and quantification of the variation of water content normal to the MEA surface cross sections. The resolution and efficiency of the detector used for the experiment were poor and the available neutron flux was low. As a result, the measurement was actually done on a thermally bonded membrane assembly that was nearly ten times thicker than that in modern fuel cells. For commercially competitive materials, a similar measurement requires a detector resolution of 10 μm or better in order to spatially resolve the water distribution. A future generation of neutron imaging techniques and technologies are being developed to achieve this.

11.2.3.3 GDL Characteristics and Water Retention

The structure of the GDL plays a large role in determining the water retention of the fuel cell. Placing a highly hydrophobic microporous layer (MPL) near the cathode catalyst helps to reduce flooding by presenting a barrier to condensed water [9]. Adding PTFE to the bulk GDL substrate can decrease or increase

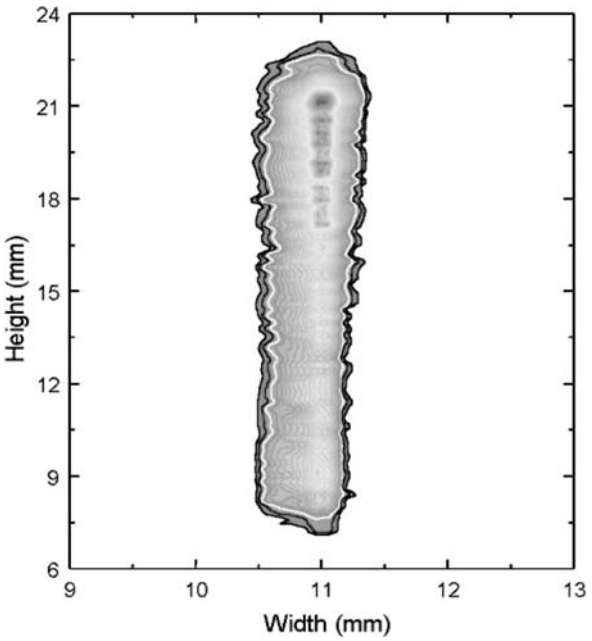

Fig. 11.5 One of the first neutron radiographs of an operating fuel cell, showing the water gradient across a 0.5 mm thick (wide) membrane, comprising several thermally bonded Nafion 117 membranes. The darker region in the membrane center indicates more water

water retention [10]. Having a broad range of pore sizes can ensure that there are sufficient pathways for reactant gas to reach the catalyst layer [11].

11.2.3.4 Characterization of Two-Phase Flow Phenomena in the Flow Field

The water removal from the fuel cell GDL and channels is a difficult process to model since it is a non-isothermal, two-phase flow system. For instance, the waste heat produced in the cathode can drive evaporation so that the fuel cell retains significantly less water at higher current production, despite the corresponding increase in water production [12]. Additionally, the operating pressure and inlet gas flows impact the condensation rate and the convection of water in the flow channels [13].

11.2.3.5 Membrane Durability

One of the failure modes of PEM fuel cells stems from dimensional changes of the polymer layers resulting from repeated drying and wetting cycles or freeze–thaw cycling. Using high-resolution neutron imaging, the effects of freezing on the formation of "frost heaves" between the GDL and MEA can be resolved [14].

Also, it may be possible to study interface defects by neutron phase contrast imaging techniques that are currently being developed (Chapter 8).

11.2.3.6 Materials for Hydrogen Storage

The success of any future hydrogen economy depends, in no small part, on the ability to develop inexpensive, state-of-the-art materials with high hydrogen storage capacity. Such targets require the search for new and improved materials. The utility of a particular material for these applications depends critically on ionic transport. Thus, the fundamental questions that must be answered in order to understand and tailor the performance of these systems are "Where do the ions go?" and "How do they get there?" Many types of materials have been tried or suggested for use as hydrogen storage media. Proper characterization of these materials requires information regarding hydrogen diffusion properties as well as the macroscopic morphologies that govern their useful properties. As shown in Fig. 11.2, neutron imaging can play a key role in assessing device performance.

11.3 Neutron Imaging Facilities and Techniques

11.3.1 Basic Principles

The quality of the image depends on a complex interplay of beam properties, sample material, neutron intensity, and temporal and spatial resolution of the detector system. For hydrogen or water, the primary form of interaction is scattering with a cross section of $0.8\times10^{-22}\,\mathrm{cm}^2$. This is nearly two orders of magnitude larger than that of aluminum, a common material used in fuel cell construction. The total transmission of neutron flux is given by the Lambert-Beer law:

$$\frac{I}{I_0} = \mathrm{e}^{-\sum_i (N\sigma t)_i}, \tag{11.1}$$

where I is the transmitted and I_0 the incident neutron flux, N is the atom number density, t is the sample thickness, and σ is the total scattering cross-section responsible for the neutron loss in the forward direction passing through the sample. Since the primary goal is to image and quantify the water content, all measurements involve the basic steps of taking a dry and wet image of the device. The wet image is normalized with respect to the dry image to determine the profile of the water thickness. The detection system typically consists of a scintillator viewed by either a charge-coupled device CCD or an amorphous silicon flat panel. The spatial resolution, which is a convolution of detector

hardware pixel resolution, geometric blur, and scintillator blooming, determines which components of the fuel cell can be identified.

The water volume can be obtained by combining the water thickness from Eq. (1) with knowledge of the area A and the liquid water attenuation coefficient, $\mu_w = N_w\sigma_w$. Since σ_w depends on neutron energy, μ_w must be measured for each beamline or spectrum and detector system used. The total uncertainty in the water thickness, δt_w, comes from both random and systematic contributions. The random uncertainty, from Poisson counting statistics, is the fundamental limit to the measurement accuracy and is estimated by:

$$\delta t_w \approx \frac{1}{\mu_w}\sqrt{\frac{2}{I_0 A T \eta}} \quad , \tag{11.2}$$

where I_0 is the incident fluence rate ($cm^{-2}\,s^{-1}$), T is the acquisition time, and η is the detection efficiency [15]. Typical random uncertainties achieved at the national institute for standards and technology (NIST) neutron imaging facility range from 1 to 10 μm.

11.3.2 Imaging Techniques

Both 2D and 3D neutron imaging are used to study water dynamics in fuel cells. Neutron tomography can provide important information about an object's internal construction and about its constituent materials. The neutron tomography technique allows one to reconstruct a 3D image of an object from the 2D neutron radiographs taken for several rotations of the object about a rotation axis (Chapter 6). Using the technique of filtered back projection (FBP), these projection images are Fourier filtered and then back-projected across planes orthogonal to the rotation axis. The result of this process is a stack of 2D reconstructions of the planes of the object, orthogonal to the rotation axis. The result of the FBP is a 3D map of the object's neutron attenuation coefficient. Subtracting the dry map from the wet map yields the 3D water profile of the fuel cell. The spatial resolution of the map is determined by the resolution of the detector system, on the order of 100 μm. Figure 11.6 shows the 3D water content of an operating fuel cell at steady state.

Because of the time required to rotate the fuel cell by 180°, neutron tomography can be used only as a steady state measurement. Often the desired information is the average water gradient going from the anode to the cathode. This "through-plane" water gradient must be imaged with higher resolution than is typical of scintillator-based detectors, since the total thickness of the PEM sandwich is only on the order of 0.5 mm. Various companies are developing new detector technologies aimed at achieving 10 μm or better resolution in neutron detection in the near future [16]. These detectors are based on microchannel plates and have been demonstrated to have resolution better than 25 μm [17] (Chapter 3). With a smaller pixel size, image acquisition time must

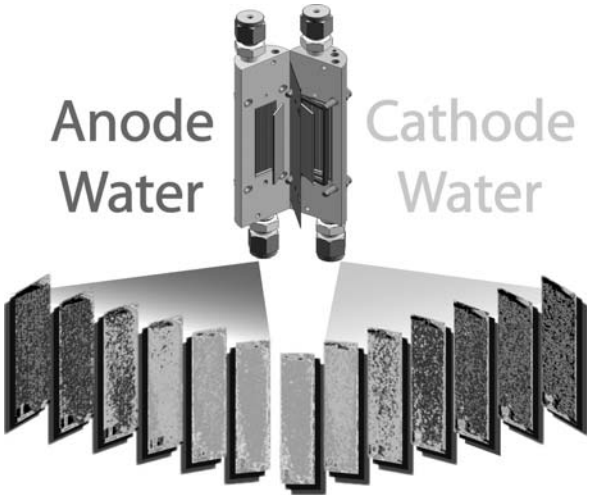

Fig. 11.6 A small fuel cell (4 cm^2) was used to demonstrate neutron tomography. The water distribution in each slice plane from the anode to the cathode shows that anode flooding is occurring in this fuel cell as a result of the thick (1 mm) gas diffusion layers. The data set was acquired within 20 min

be increased in order to maintain signal-to-noise ratios similar to those achieved with scintillators, and a typical time is similar to that of a tomography scan. While a high-resolution through-plane image yields only 2D information, it enables direct measurement of the water gradient in commercial-grade GDLs.

11.3.2.1 Phase Imaging and Other Emerging Techniques

The neutron tomography technique can be complemented by two other related imaging techniques, refraction imaging (Chapter 6) and phase contrast imaging (Chapter 8). The refraction imaging technique uses a mono-energetic neutron beam that is refracted by constituent elements in the sample. The refracted beams from different elements are spatially separated from each other by a very small amount. A single-crystal analyzer redirects this spatially separated beam away from the original direction, and a high-resolution position-sensitive detector detects the redirected beam. Since the refracted beam is now separated from the direct transmitted beam, the inherent background present in normal radiographs is eliminated, and an image with very sharp contrast is formed.

In phase contrast imaging, an image of the locally varying phase shift of a neutron beam caused by the sample is formed. Phase variation may occur because of dimensional and constituent variations, the presence of a magnetic domain structure, the presence of precipitates, or a spatial distribution of stress. The image is recorded with a high-resolution position-sensitive detector. Not

only are the bulk properties of the sample measured, but the *elemental distributions* of local inhomogenities are also observable. This technique is typically a few hundred times more sensitive than normal radiography. It is ideally suited for detecting laminate separation and minute thickness variations of polymer electrolyte layers. NIST is developing a cold neutron imaging facility that will enable research to measure the phase gradient, using a variety of such techniques, including a grating method based on the Talbot effect [18].

Ultimately, these technologies can be used as a quality control tool for fuel cell manufacturers. Fuel cells can be subjected to routine scans for the verification of proper assembly and operational characteristics. Additional resolution may be achieved using neutron point sources to magnify the neutron image of the sample.

11.4 Neutron Imaging Facilities for Fuel Cell Research

Successful applications of neutron imaging of fuel cells require access to high-intensity neutron sources and a detection system with fast temporal and high spatial resolution. Also, any large-scale comprehensive research with fuel cell and hydrogen storage devices requires an associated hydrogen support infrastructure capable of safely providing large quantities of hydrogen to these devices. The latter requirement is especially difficult for conventional steady state reactor-based neutron sources. There are facilities in the United States (NIST, PSU), Japan (JAERI, KURRI), and Europe (PSI, HMI, FRM2) that are carrying out fuel cell related research. Among these, the facility at NIST has the most developed and focused infrastructure for hydrogen economy related research. In order to give an idea of the practical considerations, a brief description of this facility follows.

The NIST neutron imaging facility is located at beam tube 2, with a direct view of the reactor core at the NIST Center for Neutron Research; a schematic layout is shown in Fig. 11.7. An aperture of diameter D (variable diameter from 0.1 cm to 2 cm) defines the beam collimation, characterized by the ratio L/D, where $L \approx 6$ m is the distance from the aperture to the detector. A 10 cm section of Bi is used to reduce the gamma-ray and fast neutron background, though it also reduces the thermal neutron fluence rate by about a factor of four from that with no filter. The typical fluence rates used range from about 2×10^6 cm^{-2} s^{-1} to 3×10^7 cm^{-2} s^{-1}. The flight path is evacuated to reduce the neutron scattering in air. The sample position sits directly in front of the detector, and there is a 5-axis manipulation table to align the object and perform tomography. There are several penetrations through the radiation shielding to allow gas lines and electrical connections to be made between the fuel cell and fuel cell test stand. The NIST test stand accurately controls the flow of hydrogen, air, nitrogen, oxygen, and helium over a wide range of flow rates [15]. The maximum current that the test stand can control is about 500 A. The inlet gases are humidified in

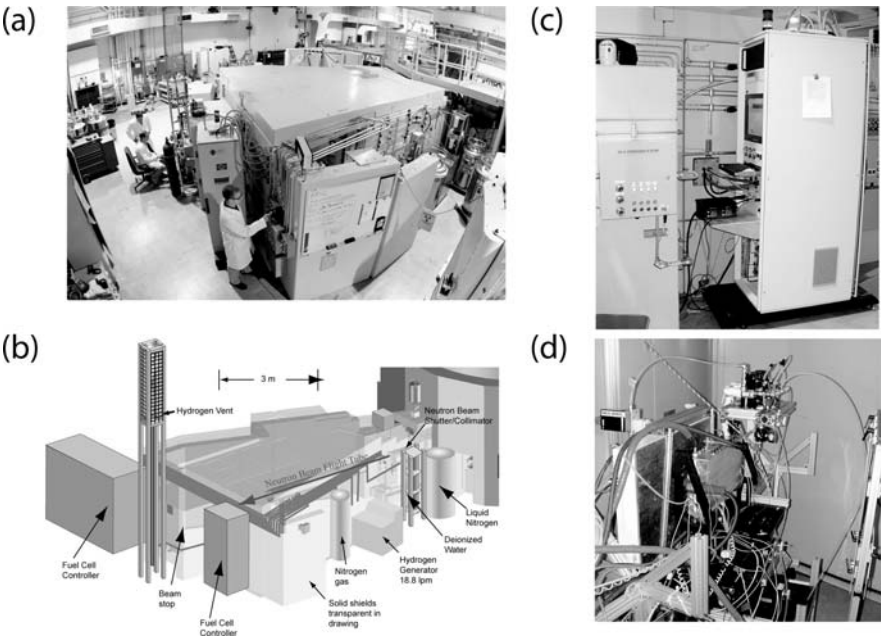

Fig. 11.7 (**a**) Photograph, and (**b**) schematic of the NIST neutron imaging facility. Also shown is (**c**) the fuel cell test stand and (**d**) the sample area with connections to a typical fuel cell

sparger bottles, and heated inlet gas lines prevent condensation. The hydrogen is supplied by a hydrogen generator so there is no stored inventory of hydrogen in the confinement building. There is an extensive set of hydrogen safety features, including several hydrogen sensors, a line pressure sensor, and flame detection in the hydrogen vent that automatically shuts down all hydrogen systems in the event of a detected emergency. Also, there is a freeze chamber, capable of controlling the temperature between –40°C and 50°C for use in freeze/thaw studies.

11.5 Examples of PEM Fuel Cell Neutron Imaging

To demonstrate the capability of 3D neutron imaging, we describe a study of a small PEM fuel cell, with an active area of 4 cm^2 (Fig. 11.6). The tomography was performed with a scintillator-based detector and, in order to measure water gradients, a 1.0 mm thick GDL on the anode and cathode were used, as well as a Nafion 117 membrane. Because of this large thickness, the diffusion through the GDL was significantly slower than in typical fuel cells, which impacts the water content. In particular, the water gradient shows that there is significant flooding in the anode.

Because of the surprising amount of anode flooding, a second experiment using the same small fuel cell was conducted to measure the water diffusion

times under different conditions. The fuel cell was operated at 0.4 V with both gas streams humidified to a relative humidity (RH) of 75 % for 2 h to ensure that the GDL saturation was at equilibrium. After this precondition, the fuel cell load was dropped. In the first case, the humidified gas flows were maintained, and in the second case the gas flows were stopped. By so doing, the efficacy of the competing GDL water transport mechanisms of capillary action versus evaporation and advection could be compared. Figure 11.8 shows the first case in which the fuel cell load was stopped but the gas flow was maintained. The water content in the GDL is seen to decline rapidly to the completely dry state within about 15 min. Figure 11.9 shows the second case where

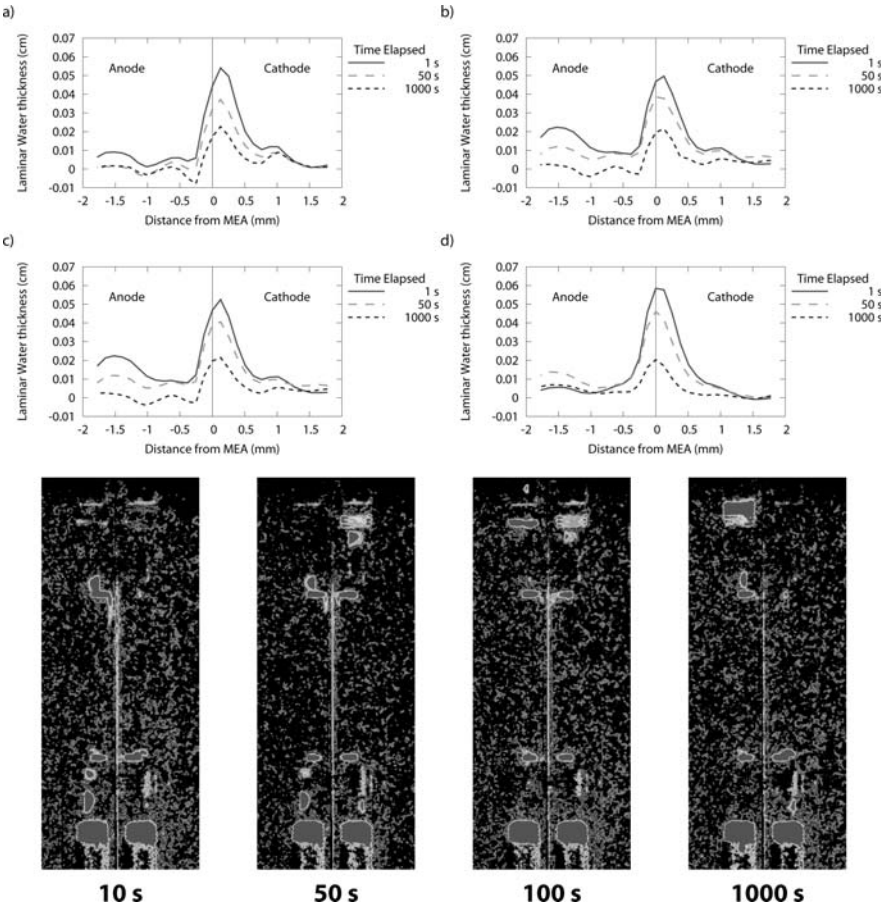

Fig. 11.8 Water transport in the GDL when the fuel cell load is stopped, but the undersaturated flows are maintained. (**A–D**) Through-plane water profiles are shown from four of the repeat measurements. The grayscale neutron images show the water profile change from a time after the load was stopped

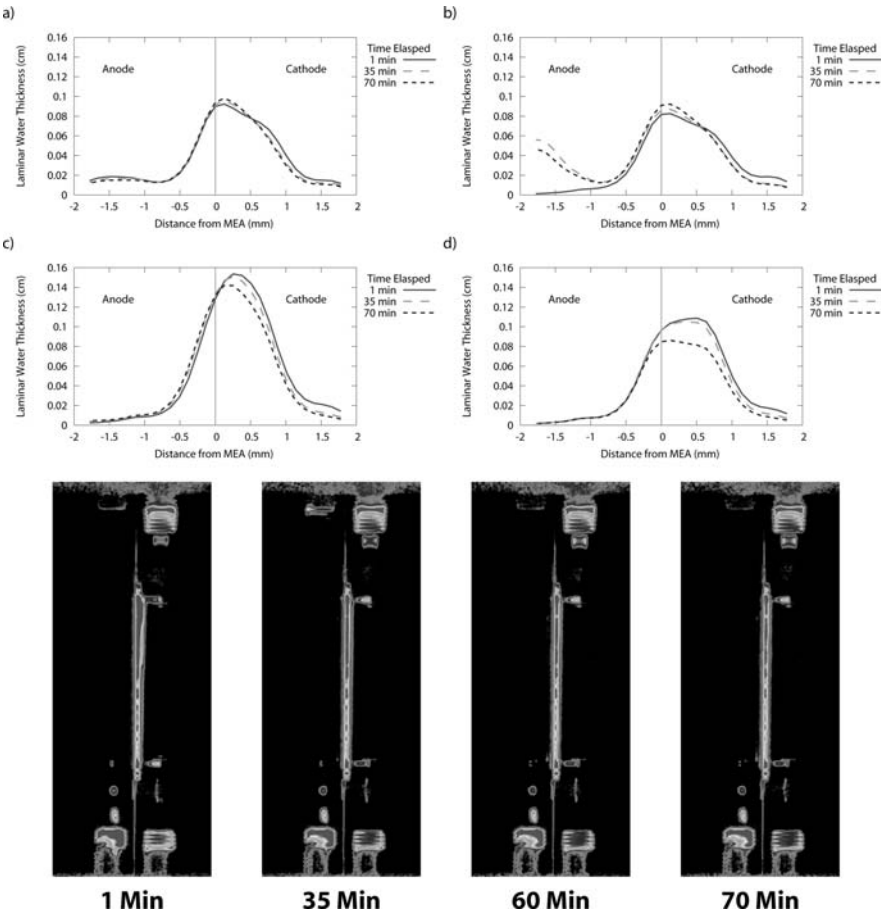

Fig. 11.9 Water transport in the GDL when the fuel cell load and the gas flows are stopped. (**A–D**) Through-plane water profiles are shown from four of the repeat measurements. The grayscale neutron images show the water profile change from a time after the load was stopped. Compared with the evaporation/advection case, the change in water content of the GDL is negligible

both the fuel cell load and gas flows were stopped. The water content of the GDL barely changes, even after 70 min, indicating that capillary action plays a smaller role than evaporation and advection in the water transport through the GDL.

11.6 Conclusion

Neutron imaging has become a powerful tool in the development of hydrogen-based alternate energy devices. It is the only technique that can study the critically important *in situ* water transport in commercial-grade fuel cells.

Today this technique is used by almost all automobile manufacturers and major fuel cell developers. By all accounts, neutron imaging research has shortened the development time of fuel cells and is providing reliable, real-time data important for optimum design and performance that was almost impossible to get only a few years ago. Though the primary focus of neutron imaging research has been on fuel cells during the last few years, it has now started to play an expanded role in the development of hydrogen storage materials and devices. It is expected that this trend will continue in the coming years. In spite of all the success that neutron imaging has enjoyed in recent years, even higher-impact research is limited by the current temporal and spatial resolution of neutron detection devices, the lack of very accurate analytical techniques, and the lack of availability of wide infrastructures for hydrogen research at various neutron facilities around the world. Fortunately, all of these issues are being aggressively pursued by various government laboratories and industrial and academic researchers. It is expected that in the very near future, both temporal and spatial resolution will improve by an order of magnitude. This, coupled with advanced methods such as phase contrast imaging, will provide much needed enhanced capabilities and open new avenues of research that are not possible today. Consequently, in the foreseeable future, neutron imaging will continue to significantly contribute to enhanced efforts to develop and commercialize pollution-free, hydrogen-powered energy devices that are the centerpieces of the emerging hydrogen economy.

References

1. Certain trade names and company products are mentioned in the text or identified in an illustration in order to adequately specify the experimental procedure and equipment used. In no case does such identification imply recommendation or endorsement by NIST, nor does it imply that the products are necessarily the best available for this purpose.
2. J. St-Pierre, *J. Electrochem. Soc.***154**, B724 (2007).
3. P. Bhandari, M. Prina, M. Ahart, R. C. Bowman, and L. A. Wade, Sizing and Dynamic Performance Prediction Tools for 20 K Hydrogen Sorption Cryocoolers in *Cryocoolers 11*, Edited by R. G. Ross, Jr. Kluwer Academic/Plenum Press, New York, pp. 541–549 (2001).
4. M. Prina, P. Bhandari, R.C. Bowman, L. A. Wade, D. P. Pearson, and G. Morgante, Performance Prediction of the Planck Sorption Cooler and initial Validation, *Advances in Cryogenic Engineering*, Vol. 47, edited by S. Breon, et al., Am. Inst. Phys., New York, pp. 1201–1208 (2002).
5. P. Bhandari, M. Prina, R.C. Bowman-Jr, C. Paine, D. Pearson, A. Nash, Sorption Coolers using a Continuous Cycle to Produce 20 K for the Planck Flight Mission, *Cryogenics* **44**, 395–401 (2004).
6. D. Pearson, R. Bowman, M. Prina, P. Wilson, The Planck Sorption Cooler: Using Metal Hydrides to Produce 20 K, *J. Alloys Compounds* **446–447,** 718–722 (2007).
7. J. P. Owejan., T. A. Trabold, D. L. Jacobson, M. Arif, and S. G. Kandlikar, *Int. J. Hydrogen Energy* **32**, 4489 (2007).
8. R. J. Bellows, M. Y. Lin, M. Arif, A. K. Thompson, and D. Jacobson, *J. Electrochem. Soc.* **146**, 1099 (1999).

9. M. Mathias, J. Roth, J. Fleming, and W. Lehnert, 'Diffusion Media for PEM Fuel Cells,' in Handbook of Fuel Cells – Fundamentals, Technology and Applications. *Fuel Cell Technology and Applications*, Vol. 3, W. Vielstich *et al.*(Eds.), John Wiley & Sons, Chapter 46 (2003).
10. R. Mukundan, J. R. Davey, T. Rockward, J. S. Spendelow, B. S. Pivovar, D. S. Hussey, D. L. Jacobson, M. Arif, and R. L. Borup, 'Imaging of Water Profiles in PEM Fuel Cells Using Neutron Radiography: Effect of Operating Conditions and GDL Composition', *ECS Trans*. **11**(1), 411 (2007).
11. K. Yoshizawa, K. Ikezoe, Y. Tasaki, D. Kramer, E. H. Lehmann, and G. G. Scherer, *ECS Trans*. **3**, 397 (2006).
12. M. A. Hickner, N. P. Siegel, K. S. Chen, D. N. McBrayer, D. S. Hussey, D. L. Jacobson, and M. Arif, *J. Electrochem. Soc*.**153**, A902 (2006).
13. M. A. Hickner, N. P. Siegel, K. S. Chen, D. N. McBrayer, D. S. Hussey, D. L. Jacobson, and M. Arif, *J. Electrochem. Soc*. **155**(4), B427–B434 (2008).
14. S. Kim, A.K. Heller, M.C. Hatzell, M.M. Mench, D.S. Hussey, D.L. Jacobson, High Resolution Neutron Imaging of temperature-driven flow in polymer electrolyte fuel cells, *American Nuclear Society National Meeting*, Anaheim, CA (2008).
15. D.S. Hussey, D.L. Jacobson, M. Arif, K.J. Coakley, and D.F. Vecchia, *In situ* fuel cell water metrology at the NIST neutron imaging facility, *Proceedings of the ASME Fuel Cell Conference*, New York, June 18–20, 2007.
16. O.H.W. Siegmund, J.V. Vallerga, A. Martin, B. Feller, M. Arif, D.S. Hussey, and D.L. Jacobson, *Nucl. Instrum. Meth. A* **579**, 188 (2007).
17. W.B. Feller, P.L. White, and P.B. White, Gamma Insensitive Highly Borated Microchannel Plates for Neutron Imaging, *Proceedings of the 8th World Conference on Neutron Radiography,* 583–591 (2008).
18. F. Pfeiffer, C. Grünzweig, O. Bunk, G. Frei, E. Lehmann, and C. David, *Phys. Rev. Lett*. **96**, 215505 (2006).